

# Impacts of including forest understory brightness and foliage clumping information from multiangular measurements on leaf area index mapping over North America

Jan Pisek,<sup>1,2</sup> Jing M. Chen,<sup>1</sup> Krista Alikas,<sup>3</sup> and Feng Deng<sup>1</sup>

Received 29 August 2009; revised 21 February 2010; accepted 30 April 2010; published 1 September 2010.

[1] A new leaf area index (LAI) data set in 10 day intervals with consideration of the understory reflectance and foliage clumping effects over North America for 1 year is developed. The data set brings effectively together measurements from multiple sensors with complementary capabilities (SPOT-VEGETATION, Multiangle Imaging Spectroradiometer, POLDER). First, the temporal consistency analysis indicated the new product is on par with other available LAI data sets currently used by the community. Second, with the removal of the background (understory in forests, moss, litter, and soil) effect on the forest overstory LAI retrieval, slightly different LAI reductions were found between needleleaf and broadleaf forests. This is caused by the more clumped nature of needleleaf forests, especially at higher LAI values, which allows more light to penetrate through the overstory canopy, making the understory more visible for equal LAI as compared to broadleaf forests. This is found over a representative set of 105 CEOS Benchmark Land Multisite Analysis and Intercomparison of Products sites in North America used for indirect validation. Third, the data set was directly validated and compared with Moderate Resolution Imaging Spectroradiometer Collection 5 LAI product using results from the BigFoot project for available forest test sites. This study demonstrates that the fusion of data inputs between multiple sensors can indeed lead to improved products and that multiangle remote sensing can help us to address effectively the issues (separating the signal from the understory and overstory, foliage clumping) that could not be solved via the means of the conventional mono-angle remote sensing.

**Citation:** Pisek, J., J. M. Chen, K. Alikas, and F. Deng (2010), Impacts of including forest understory brightness and foliage clumping information from multiangular measurements on leaf area index mapping over North America, *J. Geophys. Res.*, *115*, G03023, doi:10.1029/2009JG001138.

## 1. Introduction

[2] The importance of vegetation in studies of global climate and biogeochemical cycles has been well recognized [Sellers *et al.*, 1996]. This is especially the case with respect to carbon, with about a quarter of atmospheric carbon dioxide potentially fixed by terrestrial vegetation annually [Canadell *et al.*, 2007]. In order to estimate carbon fixation by terrestrial vegetation and exchanges between the land surface and the atmosphere, leaf area index (LAI), defined as half the total developed area of green leaves per unit ground horizontal area [Chen and Black, 1992; Jonckheere *et al.*, 2004], is required as a basic and indispensable key parameter. Since a few years, LAI has been estimated operationally from remotely sensed optical imagery at a global scale in the context of several international initiatives

that use different sensor data, methods, and approaches [Verger *et al.*, 2008]. Recent validation studies have outlined significant discrepancies among several existing LAI products and ground measurements [e.g., Abuelgasim *et al.*, 2006; Verger *et al.*, 2006; Weiss *et al.*, 2007]. These results were used by the CEOS to state that none of the available LAI products are yet performing globally within the threshold accuracy requirements for LAI around  $\pm 0.5$  [CEOS, 2006; Verger *et al.*, 2008].

[3] In the most comprehensive intercomparison study up to this date, Garrigues *et al.* [2008] investigated the performances of four major global LAI products. The best agreement between products was reached over grasslands and croplands, while significant differences could be observed over forests [Garrigues *et al.*, 2008]. Besides the quality of surface reflectances, it was suggested that the global LAI products need to be improved by better accounting for the vegetation structure, namely, the effects of background and foliage clumping.

[4] The vegetation background includes all the materials below the forest canopy such as grass, shrub, moss, leaf litter, rock, soil, and snow. [Pisek *et al.*, 2010b]. The effect

<sup>1</sup>Department of Geography and Program in Planning, University of Toronto, Toronto, Ontario, Canada.

<sup>2</sup>Also at Tartu Observatory, Tõravere, Estonia.

<sup>3</sup>Tartu Observatory, Tõravere, Estonia.

of background on the relationship between LAI and reflectance has been repeatedly pointed out [e.g., *Gemmel*, 2000; *Kuusik et al.*, 2004; *Eriksson et al.*, 2006; *Rautiainen et al.*, 2007; *Iiames et al.*, 2008; *Kobayashi et al.*, 2010]. Forest understory can vary with both space and time with its own temporal cycle in reflectance properties. These variations occur because of differences in species phenology and foliar display as well as diurnal and solar illumination through a seasonally varying overstory canopy [*Pocewicz et al.*, 2007]. Very often, the understory is spectrally similar to the overstory canopy [*Miller et al.*, 1997]. Various approaches were attempted to account for or minimize the effect of background on global LAI retrievals [*Myneni et al.*, 2002; *Deng et al.*, 2006]. However, during the validations and inter-comparisons, it has been repeatedly noted that the understory effect is still not entirely removed [*Pisek and Chen*, 2007; *Garrigues et al.*, 2008] and direct inclusion of seasonally and spatially variable forest understory information into the algorithms is desirable. On the basis of a refined methodology tested with airborne data [*Pisek et al.*, 2010b], *Pisek and Chen* [2009] produced a one-degree monthly forest background brightness data set over North America using multiangular Multiangle Imaging Spectroradiometer (MISR) data [*Diner et al.*, 1998]. However, the MISR-derived background vegetation values and their effects have not been fully incorporated into any of the global LAI algorithms or used to assess the uncertainty in their model results yet.

[5] Foliage clumping refers to the confined distribution of leaves within distinct canopy structures, such as tree crowns, shrubs, and row crops, relative to a random distribution [*Nilson*, 1971; *Weiss et al.*, 2004]. Not accounting for foliage clumping in both LAI retrieval algorithms and ground measurements leads to substantial underestimation of the LAI, especially for needleleaf forests [*Chen et al.*, 1997b]. *Chen et al.* [2005] published the first global clumping index map using multiangular POLDER-1 satellite data from ADEOS-1. However, the map application in global studies was restrained owing to limited spatial and seasonal phenology coverage, topographic effects, and a lack of evaluation with field measurements. Recently, *Pisek et al.* [2010a] expanded the spatial and temporal coverage with POLDER-3 data and devised a strategy to reduce the topographic effects with a high-resolution digital elevation model. The new clumping map was also evaluated with field observations over various biomes. While the remaining issue is a coarse resolution of the data set (~6 km of POLDER instrument in nadir view [*Deschamps et al.*, 1994]), the new map provides updated spatially explicit estimates of foliage clumping that can improve the assessment of global LAI products.

[6] The objectives of this paper are threefold: (1) to investigate with the sample LAI data set and algorithms of *Deng et al.* [2006] if information about the background from MISR and the foliage clumping from POLDER instruments can help us to reduce their effects on canopy LAI estimates and improve the quality of LAI maps; (2) to conduct an intercomparison of the new background-corrected and clumping-corrected LAI retrievals over North America with the latest version of the global Moderate Resolution Imaging Spectroradiometer (MODIS) LAI product (Collection 5 [*Myneni et al.*, 2002; *Shabanov et al.*, 2005]); and (3) to evaluate directly the new LAI maps over a set of four forest

validation sites with ground measurements from BigFoot project according to the methodology proposed by *Weiss et al.* [2007] for the validation of global LAI products. Finally, conclusions are drawn and implications of findings are discussed.

## 2. Data and Methods

### 2.1. VGT LAI Product

[7] On the basis of previous studies [*Roujean et al.*, 1992; *Chen*, 1996; *Chen and Cihlar*, 1997; *Chen and Leblanc*, 1997, 2001; *Brown et al.*, 2000; *Chen et al.*, 2002], *Deng et al.* [2006] developed a set of LAI algorithms for the purpose of deriving global LAI and the fraction of photosynthetically active radiation absorbed by the canopy ( $f_{\text{APAR}}$ ) from multiple sensors. This set of algorithms has some unique features, including the following:

[8] 1. Bidirectional reflectance distribution function (BRDF) is explicitly considered as part of the algorithms. No BRDF normalization is necessary prior to the input of reflectance values into the LAI algorithm.

[9] 2. There are separate algorithms for several structurally distinct biomes (conifer; tropical; deciduous; mixed forest; shrub; cropland, grassland, and others). The present biome is determined on the basis of the GLC2000 global land cover data set of *Bartholomé and Belward* [2005].

[10] 3. The effective rather than the true LAI is derived from spectral indices, as the effective LAI is the key input into the  $f_{\text{APAR}}$  calculations [*Fensholt et al.*, 2004]. The actual value of LAI is converted from the effective LAI using a clumping index [*Chen and Black*, 1992; *Weiss et al.*, 2004].

[11] 4. The reduced simple ratio for forests is utilized to limit the effect of understory [*Brown et al.*, 2000; *Stenberg et al.*, 2004].

[12] The SPOT-VEGETATION (VGT) data used in this study were acquired in the form of 10 day composite (S10) scenes over North America for the year 2002 from the Spot Image/VITO distribution site (<http://free.vgt.vito.be/>). The spatial resolution is 1 km, and the data are in plate carrée projection with the World Geodetic System 84 coordinate system. The VGT LAI product consists of 36 scenes that cover the whole year. The 10 day values are further subjected to a smoothing procedure [*Chen et al.*, 2006a] in order to minimize residual atmospheric effects and reconstruct a seasonal trajectory of LAI for each pixel.

[13] Inputs to the original LAI algorithms included a global land cover classification data set (GLC2000) [*Bartholomé and Belward*, 2005], reflectance and angular values from the VGT sensor, and empirical values of clumping index for different land cover types as provided by *Chen et al.* [2005].

### 2.2. Inclusion of the New Information About Understory and Foliage Clumping in the VGT LAI Algorithms

[14] The spectral signatures of the background values vary geographically as well as temporally with moisture and understory vegetation composition [*Bubier et al.*, 1997; *Rautiainen et al.*, 2007]. As the differences in spectral signatures between soil and understory vegetation are much larger than those among different soil types, *Deng et al.* [2006] decided to include all the vegetation (understory +

canopy) in the calculated LAI before a sound background information could be acquired. In carbon cycle modeling, overstory LAI and background LAI are treated differently because carbon fixed through net primary productivity has different residence times for these different vegetation components in forest ecosystems [Vogel and Gower, 1998; Rentch et al., 2003]. Prior to the multiangle remote sensing, mono-angle remote sensing did not allow differentiating between these layers of vegetation [Gemmel, 2000]. On the basis of the results of Chen et al. [2002], the background simple ratio (SR) value of 2.4 was used in all of the simulations for forest types and the development of the original VGT LAI algorithms [Deng et al., 2006]. SR corresponding to bare soil was applied in the actual LAI retrieval [Pisek et al., 2007]. In the new version of the LAI algorithms with the forest background information derived from multiangular MISR data as described in Pisek and Chen [2009], a scheme based on Chen et al. [1999] is fully adopted to adjust for the effect of the difference between the actual background  $SR_B$  and the standard background values used in model simulations ( $SR = 2.4$ ). The adjusted  $SR'$  for the pixel to be used in LAI inversion is

$$SR' = (2.4 - SR_B) \cos(\theta_v) \frac{SR_{MAX} - SR_T}{SR_{MAX} - SR_B} + SR_T, \quad (1)$$

where  $SR_{MAX}$  is the maximum SR value of the algorithm for a cover type at a view zenith angle ( $\theta_v$ ) and  $SR_T$  is the original (understory + canopy) value of SR from VGT. In equation (1),  $(SR_{MAX} - SR_T)/(SR_{MAX} - SR_B)$  represents the gap fraction at nadir [Chen et al., 1999]. This term is multiplied by  $\cos(\theta_v)$  to consider the decreasing probability in viewing the background through the canopy with increasing view zenith angle. The first term in the right-hand side of equation (1) is therefore an adjustment to  $SR_T$  to consider the variation in background brightness before it is used for LAI retrieval. This adjustment is proportional to the difference between a constant of 2.4 used in the previous algorithm and pixel-specific  $SR_B$ , assuming this ratio does not change with view and sun angles. The BRDF effect of the background is greatly minimized using this ratio. As the understory layer is accounted for in this way, the LAI retrievals correspond to the overstory effective LAI only. It must be noted the used background brightness maps are of a low one-degree resolution because of the often missing measurements in MISR 1 km observations. This is due to the cloud cover and other suboptimal atmospheric or illumination conditions [Pisek and Chen, 2009]. At the same time, the background is often similar over a wide geographic area, although small-scale variability may exist between stands of different densities in close proximity [Serbin et al., 2009; Steinberg et al., 2006]. A small uncertainty is thus present in the assessment of background at 1 km resolution while using the current background maps.

[15] The true LAI values are computed now from the effective LAI using spatially explicit values of clumping index from the ~6 km resolution updated POLDER data-derived map from Pisek et al. [2010a]. While overall the results do not differ significantly from the mean values presented in Chen et al. [2005], the expanded temporal and spatial coverage with POLDER-3 data, topographic effect removal, and limited evaluation with ground measurements

increase our confidence in the updated map. The fusion of the inputs from the three complementary sensors thus forms the new VeMP (VEGETATION, MISR, POLDER) LAI<sub>o</sub> (overstory) product analyzed in this study.

### 2.3. Validation Sites

[16] A subset from the network of sites dedicated to the intercomparison of land biophysical products, the CEOS Benchmark Land Multisite Analysis and Intercomparison of Products (BELMANIP) [Baret et al., 2006], is used in this paper. This benchmark network was designed to provide a good sampling of biomes and land surface types over the globe and brings together 404 sites (full list at [http://lpvs.gsfc.nasa.gov/lai\\_intercomp.php](http://lpvs.gsfc.nasa.gov/lai_intercomp.php)) extracted from several existing networks (Aerosol Robotic Network, FLUXNET, Validation of Land European Remote Sensing Instruments, BigFoot, and others). The VGT LAI and VeMP LAI<sub>o</sub> are first investigated over a subset of 105 sites in North America in 2002. Although ground measurements are not available for every site, the BELMANIP network is very useful to complement the direct validation presented later in the paper by providing a good sampling in both space and time. Using 105 locations over 1 year with 10 day frequency of VGT and VeMP LAI retrievals, 3780 observations are thus made available for intercomparison from each product.

[17] To perform any intercomparison or validation, the target must obviously match the same area, i.e., correspond to the same geographic location and size. Geolocation uncertainties, differences in projection systems, and point spread functions have to be accounted for [Weiss et al., 2007]. The geolocation uncertainty is not an issue here as both VGT LAI products come from the identical input data set in plate carrée grid. Considering the spatial dimension and the effect of point spread function of the VGT sensor [Fillol et al., 2006], a 3 km × 3 km support area at each site was considered for the analysis as recommended by Weiss et al. [2007]. The median LAI value over 3 × 3 pixels area was used. Using the median value instead of the average value of LAI allows removing most outliers inside the 3 km × 3 km area. In addition, using the median makes a better match with the “dominant class” if the class is assumed to be the main driver of variability between pixels in the 3 km × 3 km area [Verger et al., 2008].

[18] The biome information about the site location was retrieved from the GLC2000 data set classified into six biomes. As the VGT LAI/VeMP LAI<sub>o</sub> products use the identical biome information, the used biome classification will not introduce any additional bias.

[19] The direct validation of the new VeMP LAI<sub>o</sub> product and intercomparison of seasonal trajectories with the LAI results from MODIS Collection 5 are carried out over four forest sites from the BigFoot project [Gower et al., 1999; Cohen et al., 2006a]. The four sites with available Enhanced Thematic Mapper Plus (ETM+) LAI maps for 2002 are CHEQ, a mixed forest of northern hardwoods and aspen at Chequamegon, Wisconsin, USA [Burrows et al., 2002]; METL, a temperate ponderosa pine forest with a sparse understory of bitterbrush and bracken fern at Metolius, Oregon, USA [Law et al., 2001]; HARV, Harvard Forest with ground covered predominately by litter in Massachusetts, USA [Magill et al., 2004]; and NOBS, Northern Old Black Spruce site with understory vegetation of feather

moss, Labrador tea, and *Vaccinium* spp. in Manitoba, Canada [Cohen *et al.*, 2003]. ETM+ LAI estimates at each site were directly linked to the field measurements using methods described by Gower *et al.* [1999] and Cohen *et al.* [2006b].

[20] The field measurements can be derived from several devices and interpretation techniques, and may provide estimates of effective LAI values [Weiss *et al.*, 2004] or true LAI values when leaf clumping is accounted for [Chen *et al.*, 2006b]. The most accurate measurement is achieved using destructive samplings for foliage element estimates, and locally calibrated allometric relationships to scale these estimates over plots [Chen *et al.*, 1997b; Jonckheere *et al.*, 2004]. The allometric method was applied at the NOBS site; optical analyzer LAI-2000 (LI-COR, Lincoln, Nebraska, USA) was used at the other sites [Cohen *et al.*, 2006b]. Additionally, Law *et al.* [2001] measured clumping index at the METL site. NOBS and METL estimates thus provide information about true LAI, while CHEQ and HARV retrievals refer to effective LAI only, instead. LAI of the background was not included in the measurements [Cohen *et al.*, 2006b; Law *et al.*, 2001].

#### 2.4. MODIS Collection 5 LAI Product

[21] MODIS Collection 5 products were acquired in a form of ASCII subsets over the study sites from the Distributed Active Archive Center (DAAC) database of Oak Ridge National Laboratory (<http://daac.ornl.gov/MODIS/>). Collection 5 is marked by few changes in the LAI algorithms to improve the quality of LAI retrievals and their consistency with field measurements. The acquired MODIS LAI Collection 5 product is composited every 8 days using a main retrieval algorithm based on a three-dimensional radiative transfer model tuned for eight (up from six used in the previous collections) main biome classes [Shabanov *et al.*, 2005]. New look-up tables (LUTs) were used to compare observed and modeled red and near-infrared bidirectional reflection factors for a combination of canopy structures, leaf optical properties, and soil/background patterns that represent an expected range of typical conditions for a given biome type [Knyazikhin *et al.*, 1998a, 1998b; Myneni *et al.*, 1997]. Under optimal circumstances, this LUT method is used to achieve inversion of a stochastic three-dimensional (3D) radiative transfer model [Shabanov *et al.*, 2005]. The output then represents a mean LAI value over the set of acceptable solutions for which simulated and measured MODIS surface reflectances differ within specified levels of uncertainties [Myneni *et al.*, 2002]. In contrast with the VGT/VeMP LAI algorithms of Deng *et al.* [2006], the effect of foliage clumping is supposed to be incorporated indirectly in the formulation of the extinction and the differential scattering coefficients of the stochastic 3D radiative transfer model [Myneni *et al.*, 1997]. If the main algorithm fails, a backup procedure is used to estimate LAI from biome-specific LAI-normalized difference vegetation index relationships [Myneni *et al.*, 1997]. The backup algorithm produces LAI retrievals of lower accuracy [Yang *et al.*, 2006a], mostly because of residual clouds and poor atmospheric correction [Wang *et al.*, 2001]. It is recommended to use only the retrievals from the main algorithm in validation/intercomparison studies [Yang *et al.*, 2006a]. The information about the algorithmic origin of

the retrieved MODIS LAI values was acquired along with the subsets. Only the values retrieved with the main algorithm were selected for the comparison with VGT LAI products and BigFoot results.

### 3. Indirect Validation

[22] Indirect validation consists of evaluating the performances of different products, without comparing them to actual ground measurements [Weiss *et al.*, 2007]. The temporal continuity and consistency of VGT LAI and VeMP LAI<sub>o</sub> is investigated first. Next, we compare the statistical distributions for several biome classes. The understory effect, its dependency on the canopy closure, and the LAI corrections using the forest background information from MISR are documented and illustrated on example sites.

#### 3.1. Temporal Consistency

[23] Seasonal variation patterns of remotely sensed surface parameters can first provide quality assurance of the LAI products [Cihlar *et al.*, 1997]. Apart from abrupt changes in land use such as fire or flooding, vegetation structure variables such as LAI vary continuously with time. The incremental nature of biomass production and allocation processes from which the LAI results leads to a slow variation of this variable. A smooth temporal course of a LAI product is therefore expected. The original VGT LAI product was characterized by relatively smooth seasonal trajectories with no gaps, which is required for most applications, including investigations on global biochemical cycles and climate [Buermann *et al.*, 2001]. Preservation or improvement of the temporal consistency in the VeMP LAI<sub>o</sub> data set would be thus desirable.

[24] Temporal consistency was evaluated by the smoothness level of the temporal profiles over 105 BELMANIP sites in 2002. Following Weiss *et al.* [2007], to qualify the “smoothness” of products, the difference between the LAI(*t*) product value at time *t* and the mean value between the two bracketing dates was computed:

$$\delta = (1/2(\text{LAI}(t + \Delta t) + (\text{LAI}(t - \Delta t))) - \text{LAI}(t), \quad (2)$$

where  $\Delta t$  is the temporal sampling interval. Difference  $\delta$  is computed only if the two bracketing LAI values exist. The smoother the temporal evolution, the smaller the  $\delta$  difference should be.

[25] Results (Figure 1) show that the original VGT LAI product had a very smooth temporal profile with no  $\delta$  values exceeding  $\pm 1$ . This suggests that the possible noise in the LAI algorithm outputs is effectively tackled by the cubic spline seasonal smoothing procedure by Chen *et al.* [2006b]. The dissymmetry observed for higher LAI values is due to the low probability of getting an LAI value at time  $t + \Delta t$  and  $t - \Delta t$  when LAI(*t*) is high. The understory-corrected VeMP LAI<sub>o</sub> product displays even smoother behavior (Figure 1) with residues of only two outliers exceeding  $\pm 0.5$ . The VeMP LAI<sub>o</sub> thus shows improved temporal consistency. Inclusion of vegetation understory information from MISR and clumping index values from POLDER into the LAI algorithms does not introduce any signs of abrupt changes in the temporal profiles of overstory LAI profiles.

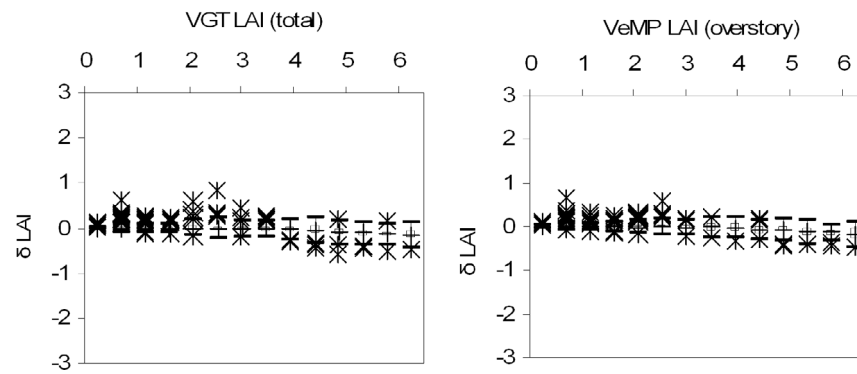


**Figure 1.** Box plot of  $\delta$  value as a function of  $\text{LAI}(t)$  value for (left) VGT LAI and (right) VeMP LAI<sub>o</sub> products. The horizontal line in the box indicates mean and median values. The box contains 50% of the data, black lines show the 95% confidence interval, and stars represent outliers.

[26] To put these results into perspective, we compare them with other products. *Weiss et al.* [2007] reported the residues of MODIS LAI temporal profiles to vary between  $-3$  and  $3$ . The root-mean-square error between  $\text{LAI}(t)$  and the two bracketing dates is also lower ( $0.07$ ) for VeMP LAI<sub>o</sub> than for Carbon Cycle and Change in Land Observational Products from an Ensemble of Satellites (CYCLOPES) ( $0.13$ ) and MODIS ( $0.58$ ), although *Weiss et al.* [2007] were carrying out the comparison over the full BELMANIP data set during the period 2000–2003. At the same time, little LAI variability between the years was observed, and the numbers can thus be considered to be comparable. The maximum VeMP LAI<sub>o</sub> value was over  $8$  over the subset of 105 BELMANIP sites. This signifies the new product is also capable of estimating the LAI values over a broader range than MODIS is ( $\text{LAI} < 7$  [*Shabanov et al.*, 2005]) or CYCLOPES ( $\sim 5$  [*Baret et al.*, 2007]).

### 3.2. Statistical Distributions per Biome

[27] Histograms of VGT LAI/VeMP LAI<sub>o</sub> product values were investigated for each of the five present main biome types used as an input into the VGT-based LAI algorithms. The values were sampled again as medians over the  $3 \times 3 \text{ km}^2$  areas of 105 BELMANIP sites in North America in 2002.

[28] Histograms of  $\text{LAI}/\text{LAI}_o$  values (Figure 2) show consistent distributions across all biomes between the two products derived from the same original VGT data. The histograms are identical for grasslands, croplands, and shrubs (Figure 2), as the vegetation understory was considered only in the case of forest biomes. The small reduction around LAI of  $2.5$  for shrubs in Figure 2 is caused by the heterogeneous nature of GLC2000 land cover classification over few BELMANIP sites, where some of the pixels over the  $3 \times 3 \text{ km}^2$  area belonged to forest biomes. Overall, the removal of the understory effect reduced the overstory LAI and shifted the value of the median slightly to lower values. The highest share of LAI values close to zero in all histograms is caused by considering the values from the whole year including the winter season. Overall, the distributions over non-forest biomes are in good agreement with the results for other products published elsewhere [*Verger et al.*, 2008]. *Garrigues et al.* [2008] also observed the best agreement between various LAI products over non-forested biomes.

[29] For the needleleaf forest (Figure 2), the increased number of VeMP values in the range of LAI  $1$ – $2$  is caused by the shift of the values from both the lower and higher values in the original VGT LAI. The forest background brightness maps produced from MISR by *Pisek and Chen* [2009] capture the presence of the snow on the ground in the winter with SR close to  $1$ . As this value is lower than the constant background SR value used in the VGT LAI algorithms to characterize bare soil, the new VeMP LAI<sub>o</sub> values can be actually higher than in VGT LAI product. The other addition to the increased number of values in the LAI range of  $1$ – $2$  in VeMP comes from the removal of the understory enhancement of LAI values during the main growing season.

[30] Differences between the distributions over both broadleaf and mixed forest biomes show similar characteristics of the consistent shift from higher LAI values of VGT to slightly reduced values (by LAI  $0.5$ – $1$ ) of VeMP. It is encouraging to see that this reduction corresponds to field measurements of understory LAI at various locations over North America found in the literature [*Miller et al.*, 1997; *Iiames et al.*, 2008; *Sonnentag et al.*, 2007; *Serbin et al.*, 2009].

### 3.3. Changes of Forest Overstory LAI with Canopy Closure and Time

[31] Scatterplots between VGT LAI products were generated to better describe their agreement and/or differences. This comparison was applied to 105 BELMANIP sites, using the median value computed over the  $3 \times 3 \text{ km}^2$  extent during the year 2002. Only the results over the forest sites are shown (Figure 3), as the scatterplots for grasslands, croplands, and shrubs form 1:1 line.

[32] The LAI<sub>o</sub> values are corrected over the full LAI range with the smaller reductions toward higher LAI values as the canopy closure increases and the understory becomes less visible. The new VeMP product thus still clearly keeps the wide range of LAI up to  $8$  over the BELMANIP needleleaf and mixed forest sites (Figure 3). The width of the reductions along the 1:1 line in the scatterplots also indicates a similar understory effect from overstory LAI of  $2$  to  $\sim 4$ . While the absolute value of the LAI reduction might be the same, the relative reduction value to the total LAI will change, being more pronounced over less dense or more

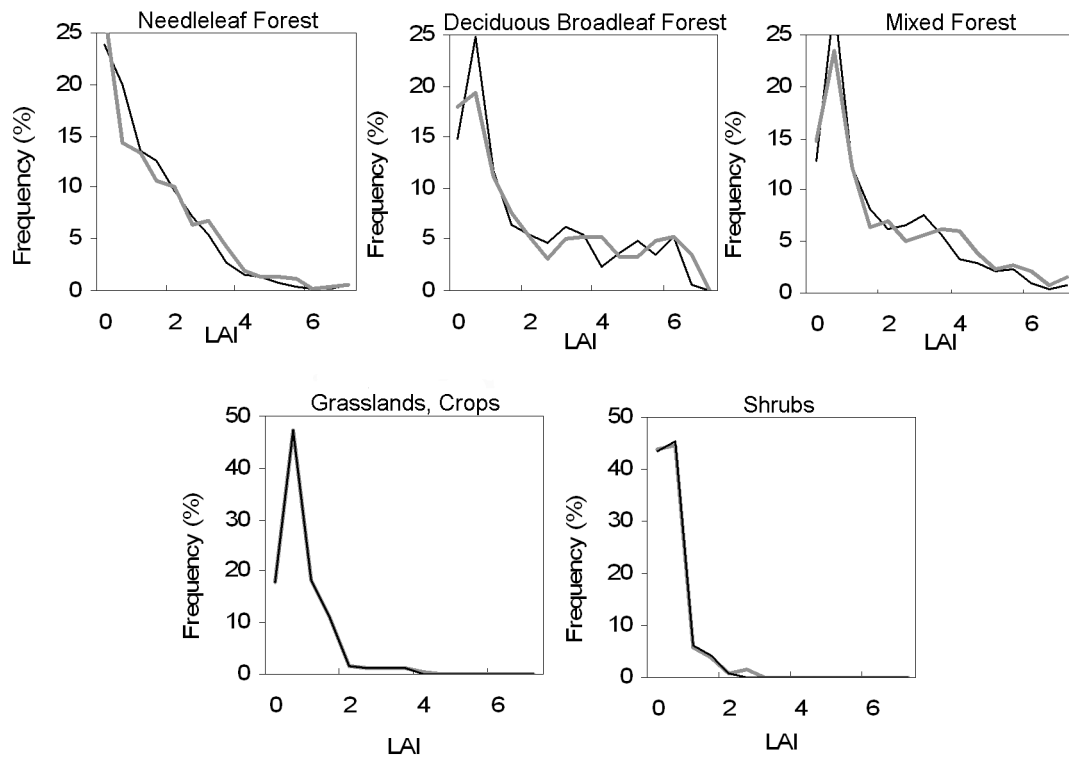


**Figure 2.** Histograms of VGT LAI (gray thick line) and VeMP LAI<sub>o</sub> products (black line) for the main biome classes. Results are computed over 105 BELMANIP sites,  $3 \times 3 \text{ km}^2$  during the period from January to December 2002 (3780 observations).

clumped stands with plenty of penetrating light to sustain abundant understory vegetation contributing to the total stand reflectance [Goward *et al.*, 1994].

[33] The relative median LAI reduction and its distribution with the total LAI are different between needleleaf and broadleaf forests (Figure 4). The median LAI reduction reaches the highest values around LAI of 3 for broadleaf forests. This coincides with the most optimal conditions for the understory vegetation growth as revealed by the analysis of the forest understory from MISR by Pisek and Chen [2009]. The needleleaf forests experience the highest LAI

reductions at LAI greater than 3 (Figure 4). This is made possible by the more clumped foliage of the needleleaf forests [Chen *et al.*, 1997b], which allows for more light penetration through the overstory and makes the understory more visible than for the less clumped and more uniform broadleaf type [Gower *et al.*, 1999]. However, overall, the higher LAI reductions are reached for broadleaf forests. This points to a more vigorous understory layer in broadleaf forests than in the case of the needleleaf forest understory, which is in agreement with previous studies [Goward *et al.*, 1994; Serbin *et al.*, 2009].

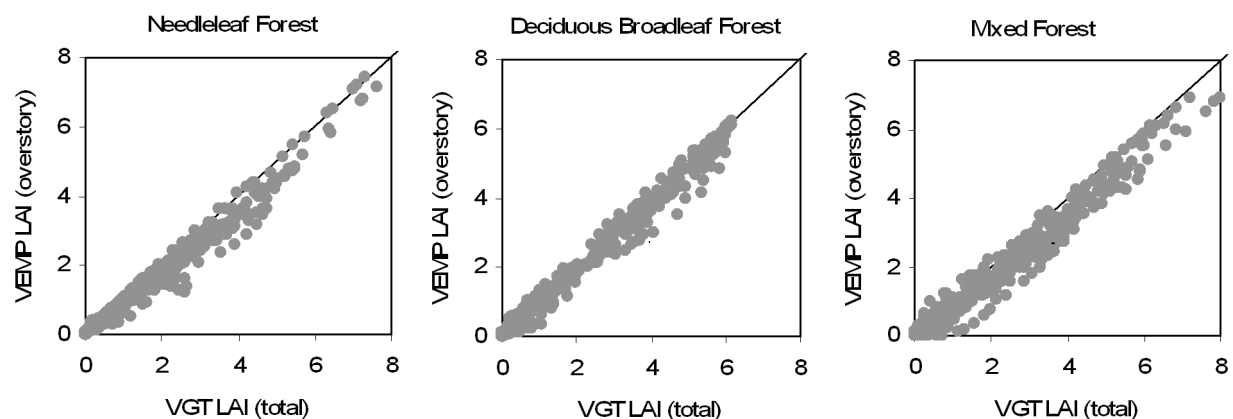


**Figure 3.** VGT LAI versus VeMP LAI<sub>o</sub> as a function of the forest biome classes over 105 BELMANIP sites.

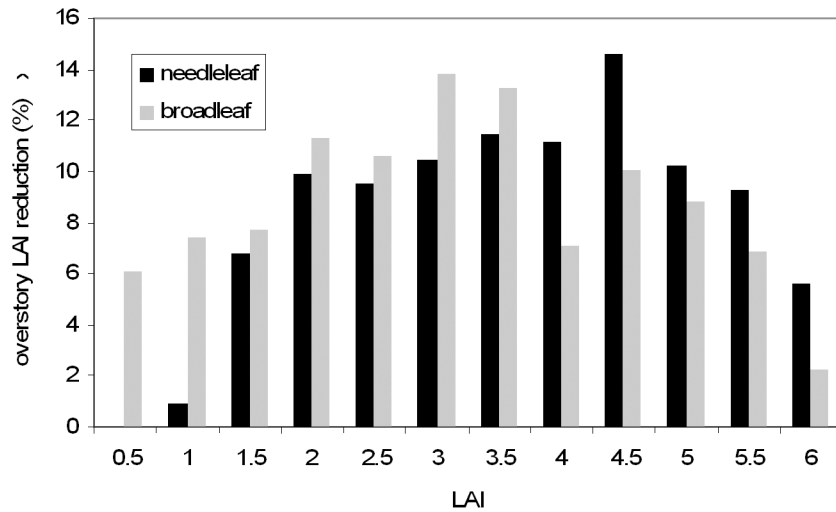


**Figure 4.** Distribution of median LAI reductions in percent from the original VGT LAI values sorted by LAI.

[34] To better document the temporal behavior of LAI products, we present time courses over two sites with different biomes: BOREAS SOA (Southern Old Aspen) corresponds to a boreal broadleaf forest with hazelnut understory [Chen *et al.*, 1997a], and a FLUXNET site in the British Columbia (BELMANIP ID 83) represents a needleleaf forest according to the GLC2000 land cover classification. These sites were chosen since they represent a typical behavior over other BELMANIP sites, and illustrate well the understory effect, its removal and remaining issues of the seasonal LAI mapping.

[35] The FLUXNET site in British Columbia presents a simple seasonal trajectory with a broad peak of constant overstory LAI values in summer (Figure 5). The forest background is contributed by LAI close to 1 in the original

VGT LAI estimates in the middle of the summer when the understory is the greenest. The clumped needleleaf overstory with LAI around 2 allows enough light to penetrate to the ground and sustain a vivid understory layer. A broad peak in summer months such as that in the case of VeMP LAI<sub>o</sub> would be expected in the case of boreal needleleaf forests, as an average leaf turnover (total foliage mass/new foliage mass) for needleleaf foliage is slow from ~4 years [Chen, 1996] up to 12 years [Gower *et al.*, 1997]. The results indicate that the seasonality in understory vegetation can indeed partly explain the observed vegetative cycles over boreal needleleaf stands recorded with remotely sensed LAI data [e.g., Yang *et al.*, 2006b]. The LAI values drop to zero values in the winter months according to both VGT LAI/LAI<sub>o</sub> products. The drop of LAI toward 0 in winter is

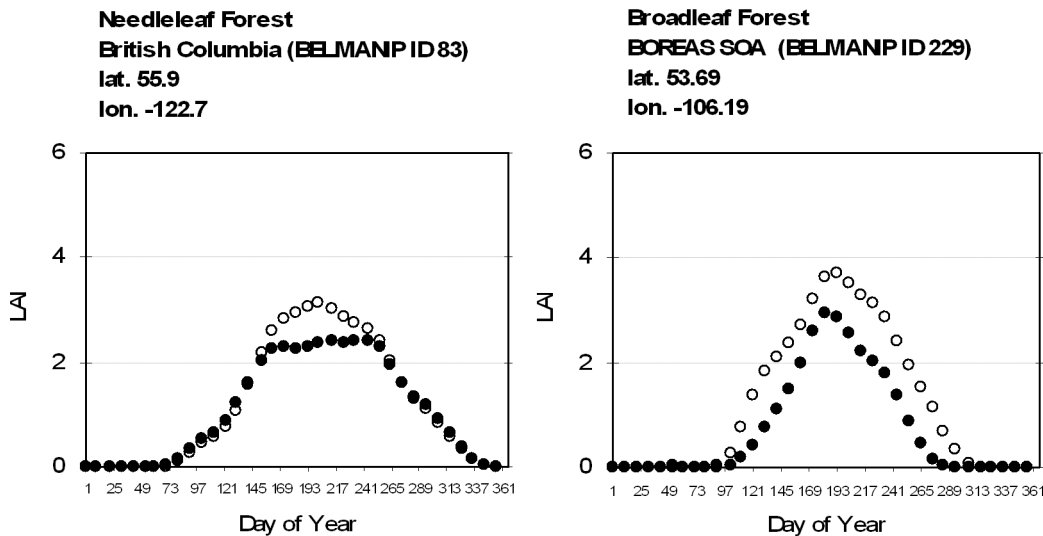


**Figure 5.** Temporal evolution of original VGT LAI (open circles) and VeMP LAI<sub>o</sub> (solid circles) in 2002 over two 3 × 3 km<sup>2</sup> sites.

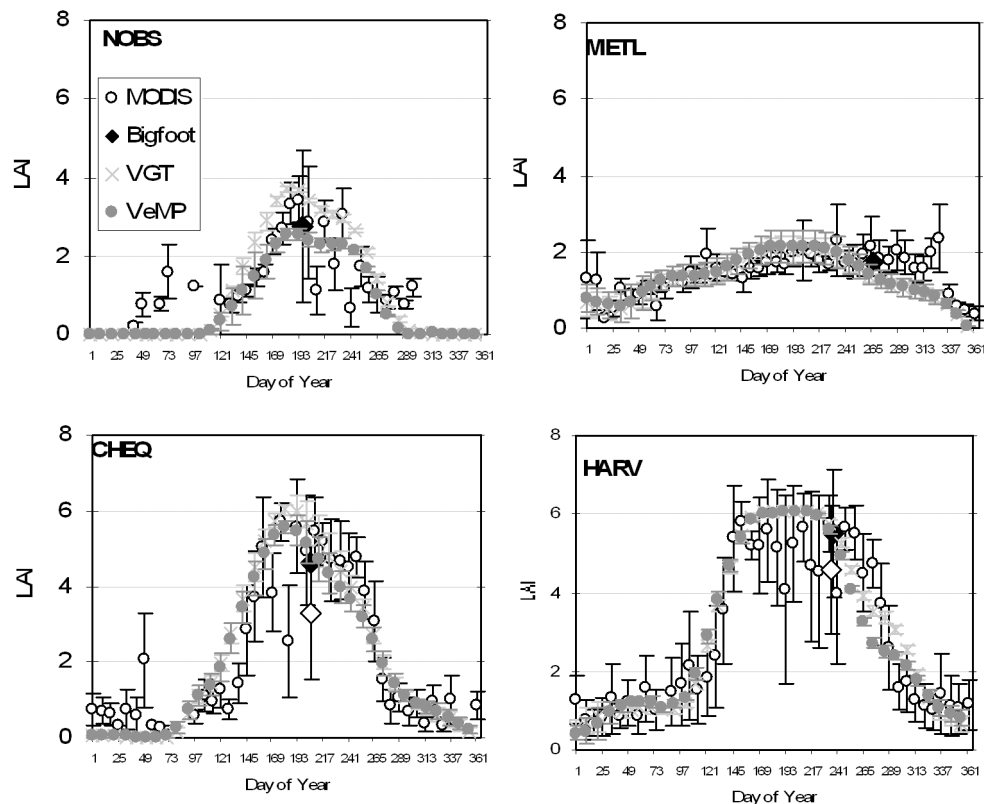


**Figure 6.** VeMP (overstory)  $LAI_o$ , original VGT LAI, and MODIS Collection 5 2002 LAI trajectories for BigFoot sites. Means and one standard deviation values are shown. BigFoot data are shown as diamonds. Black diamond signalizes true, clumping-corrected LAI value; white diamond marks effective LAI.

not expected for evergreen needleleaf forests. Previously, Yang *et al.* [2006a] and Cohen *et al.* [2006b] identified poor illumination conditions, extreme solar zenith angles, snow and cloud contamination, and the signal from the understory as the main factors for the similarly poor performance of the MODIS LAI product at high latitudes. Here the signal from the snow-covered understory clearly does not alleviate the problem. Another important factor might be then the lower levels of chlorophyll content in needles in winter [Lundmark *et al.*, 1988; Strand and Lundmark, 1995; Zhang *et al.*, 2008].

[36] Results for the SOA site indicate the beginning of the leaf emergence about day of year (DOY) 113 (Figure 5). This is in very good agreement with an estimate of DOY 110 by Chen *et al.* [1997a] from field measurements in the area. The hazelnut understory clearly forms an important part of the total LAI during the whole growing season. The VeMP  $LAI_o$  reaches a peak median LAI value of 2.95 in mid-July. This corresponds with the maximum aspen overstory LAI value of 2.88 in the meteorological footprint of the tower at the site suggested by Chen *et al.* [1997a]. Figure 5 shows a quite early start of leaf senescence with  $LAI_o \sim 2$  by DOY 230 (middle August). Previously, Serbin *et al.* [2009] observed the mean onset of senescence on DOY  $253 \pm 10$  days in the BOREAS study area for 2004–2006. The difference can be explained by a very dry summer of 2002 with very little precipitation over the area. The

drought might have sped up the leaf senescence process in that year.

#### 4. Direct Validation and Comparison with MODIS Collection 5 LAI Product

[37] In this section, the medians of the VeMP  $LAI_o$  estimates were compared with MODIS Collection 5 and direct ground measurements of effective or true LAI over four  $7 \times 7$  km<sup>2</sup> forest sites from the BigFoot project in 2002 (Figure 6). The methods used to scale up local measurements to the ETM + site level maps are described in Cohen *et al.* [2003, 2006b]. Note that ground measurements could be derived from several devices and interpretation techniques, and may provide estimates of effective LAI values or true LAI values when the foliage clumping is accounted for [Chen *et al.*, 2006b].

[38] Results show the VeMP  $LAI_o$  follows similar seasonal trajectory over the NOBS site to the one in Figure 6 over another needleleaf forest. The BigFoot LAI over the site for DOY 195 (23 June 2002) is 2.74; the VeMP retrieval for DOY 192 is 2.54 (relative error [RE] = 7.6%) and 3.43 (RE = 24.7%) for DOY 193 from MODIS Collection 5. The NOBS BigFoot LAI value refers to the true (clumping accounted) LAI, because allometry method was used in the field [Cohen *et al.*, 2006b]. The flat summer peak in VeMP  $LAI_o$  profile seems more reasonable than the strong unimodal (albeit similarly close to ground truth data) trajectory of the original VGT LAI product over the NOBS site, shown in

*Pisek and Chen* [2007]. The spurious performance in the winter half of the year over needleleaf forests still remains the issue for both products.

[39] The METL site offers another possibility of comparing the LAI products for forest sites with rather low true LAI. Similar to NOBS, the VeMP LAI<sub>o</sub> underestimates (RE = 15.9%) and MODIS Collection 5 overestimates (RE = 25.9%) the field-measured LAI. MODIS Collection 5 shows an improved stabilized seasonal trajectory over METL to the result from the previous Collections 3 and 4 [*Cohen et al.*, 2006b]. The improved MODIS trajectory seems more realistic with the seasonal dynamics at the site [*Law et al.*, 2001].

[40] Both products seem to overestimate strongly the BigFoot LAI value for the CHEQ site (VeMP RE = 57.2%; MODIS Collection 5 RE = 65.8%). However, the BigFoot LAI corresponds to the effective LAI as the field measurements were carried with LAI-2000 instrument and the clumping index was assumed to be unity [*Burrows et al.*, 2002]. After applying the clumping correction for the mixed forest from the results of *Pisek et al.* [2010a], the true LAI for the site is 4.58 (Figure 6, CHEQ), and the RE is reduced to 13.3% for VeMP and 19.4% for MODIS Collection 5 for the closest DOY LAI retrievals, respectively.

[41] The dense overstory of the broadleaf/mixed forest at HARV during the summer dominates the reflectance signal. The VeMP LAI<sub>o</sub> values at HARV in Figure 6 do not differ substantially from the original VGT retrievals shown in *Pisek and Chen* [2007]. The BigFoot estimates correspond to the effective LAI [*Cohen et al.*, 2006b]. Corrected for the clumping, the RE of the VeMP product is only 4.2%, and it is 4.5% for MODIS Collection 5. This result agrees with *Shabanov et al.* [2005], who reported an improved performance of the Collection 5 over HARV with an increased number of retrievals from the main algorithm. Interestingly, in contrast to NOBS, both products seem to be capable of delivering reasonable LAI retrievals (LAI ~ 0.5–0.8) at HARV during the winter. However, the seasonal trajectory of MODIS Collection 5 can still show unstable behavior. The instability is not present in the VeMP LAI<sub>o</sub> product, partly on account of the application of the locally adjusted cubic-spline capping method of *Chen et al.* [2006b] to minimize the residual cloud effects.

[42] After the indirect validation, the VeMP LAI<sub>o</sub> product thus delivers improved outputs over the selected forest sites with direct ground measurements as well. The results may indicate a level of performance superior to both MODIS Collection 5 and the original VGT LAI product analyzed by *Pisek and Chen* [2007]. The VeMP LAI<sub>o</sub> product meets the threshold accuracy requirements by CEOS [*Morisette et al.*, 2006] for LAI ~ 0.5 at all four sites. This was not the case of the original VGT LAI product [see *Pisek et al.*, 2007; *Pisek and Chen*, 2007]. Finally, also note that the standard deviation is very low for the new VeMP LAI<sub>o</sub> product, whereas it can be significant for some of the sites for MODIS. However, more validations are needed to see if the accuracy is maintained for other sites.

## 5. Spatial Variation of the Difference Between VGT and VeMP LAI Over North America

[43] Both VGT LAI and VeMP LAI<sub>o</sub> maps over North America from June 2002 are shown in Figure 7 to provide

an overall picture about the spatial distribution of LAI reductions at the onset of the growing season by accounting for understory effect in VeMP LAI<sub>o</sub>. Differences between the two maps can be observed most clearly in a boreal region. The largest relative differences between the two maps (up to  $\delta$  LAI over 1) correspond to regions with low to intermediate canopy cover. The fraction of radiation reaching the forest floor under these conditions can stimulate the understory development that can contribute to the overall signal observed [*Bond-Lamberty and Gower*, 2007; *Ross et al.*, 1986]. The reductions in LAI might not appear very large. It must be remembered, as mentioned in section 2.2, that a partial understory signal was already considered during the development of VGT LAI algorithms of *Deng et al.* [2006]. In that sense, the difference between the two maps in Figure 7 corresponds to the additional reduction in LAI due to the more abundant understory vegetation as mapped by MISR [*Pisek and Chen*, 2009] than the one assumed during the original LAI algorithm development by *Deng et al.* [2006]. Furthermore, the relative contribution of the understory LAI to total LAI will also decrease with higher overstory LAI such as in Ontario, Quebec, and the eastern United States (Figure 7), as the canopy closure becomes a limiting factor for the understory growth and its contribution to the total observed signal [*Lang et al.*, 2007; *Serbin et al.*, 2009]. Albeit not very large, the relative differences between the various products, as illustrated in the previous sections and in Figure 7, correspond to the range of overestimations in global LAI products observed recently by *Garrigues et al.* [2008] or *Kobayashi et al.* [2010].

## 6. Conclusions

[44] A new data set of LAI in 10 day intervals, corrected for understory and foliage clumping effects over North America, is discussed in this article. The new VeMP data set brings effectively together measurements from multiple sensors with complementary capabilities (VEGETATION, MISR, POLDER). This strategy follows the calls for fusion of various sensor measurements to improve LAI products and to address the uncertainties in the current LAI products, namely, effects of the understory and foliage clumping on the canopy LAI estimates [*Garrigues et al.*, 2008], in order to satisfy the requirements for global biochemical and climate modeling [*Bonan*, 1993; *Sellers et al.*, 1996].

[45] First, we evaluated the temporal consistency of the VeMP LAI<sub>o</sub> product. The analysis indicated the new product is on par with, if not better than, other available LAI data sets currently used by the community. Second, we showed that the LAI reductions were slightly different between needleleaf and broadleaf forests after removing the forest background contribution. This is caused by the more clumped nature of needleleaf forests that allow easier penetration of light through the canopy, making the understory more visible. This difference is found to be larger at higher LAI values. This evaluation was made over the subset of 105 BELMANIP sites in North America used for indirect validation. *Kobayashi et al.* [2010] recently concluded that, despite the importance of clumping, the understory is the more crucial parameter to derive correct LAI<sub>o</sub> estimates. In this paper we showed that the foliage clumping itself can greatly influence the impact of understory as well. Third, the

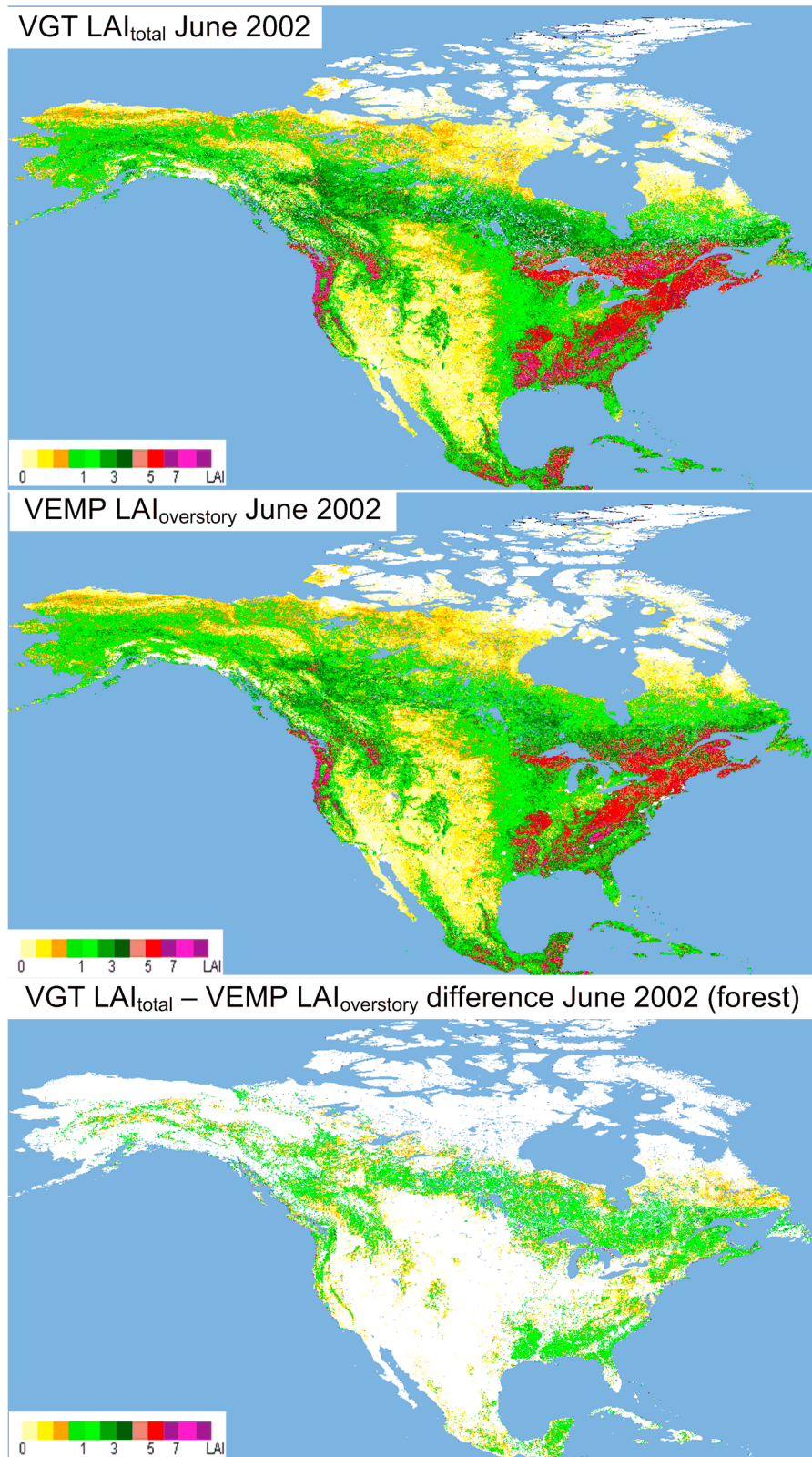


**Figure 7.** Color-coded maps of (top) VGT LAI and (middle) VeMP LAI<sub>o</sub> fields and (bottom) their difference over forested areas over North America since July 2002.

data set was directly validated using results from the well-established BigFoot project and compared to another LAI data set (MODIS Collection 5) widely used by the community over the four forest sites. The VeMP product meets the threshold accuracy requirements by CEOS [Morissette et al., 2006] for LAI  $\sim 0.5$  at all four sites. At the same time, the importance of accounting for the clumping index both in the remotely sensed and field measurements data is stressed in order to deliver comparable and true LAI estimates.

[46] The new VeMP data set still has its limitations. The spurious performance of the various LAI products in winter, over needleleaf forests in particular, remains an important issue. Next, the current input background maps are of coarse 1 degree resolution and the uncertainty about the small-scale variation of the understory is not entirely removed. Higher-resolution background brightness maps would be desirable. This issue will be addressed in depth in future research. Similarly, higher-resolution 1 km maps of clumping index would also be of benefit to other LAI products such as CYCLOPES [Baret et al., 2007]. Unfortunately, the POLDER-based  $\sim 6$  km resolution map is the only available global map as of now. Through this study, we encourage the development of new multiangle sensors at a higher resolution than POLDER.

[47] In this study, we demonstrated that physically based fusion of data from multiple sensors can indeed lead to improved products and multiangle remote sensing can help us to address effectively the issues that could not be resolved via the means of the conventional mono-angle remote sensing.

[48] **Acknowledgments.** This study is supported by the Natural Science and Engineering Council of Canada (Discovery Grant) and a student assistantship to the first author by the Centre for Global Change Science at the University of Toronto. We greatly appreciate the efforts of Warren Cohen, David Turner, Stith Gower, Steven Running and Diane Wickland of the BigFoot project. We also want to thank the DAAC database of Oak Ridge National Laboratory for providing the MODIS ASCII subsets. L. Erin Quinn helped with English style corrections. We thank three anonymous reviewers for their constructive critique.

## References

- Abuelgasim, A. A., R. A. Fernandes, and S. G. Leblanc (2006), Evaluation of national and global LAI products derived from optical remote sensing instruments over Canada, *IEEE Trans. Geosci. Remote Sens.*, *44*, 1872–1884.
- Baret, F., J. Morissette, R. A. Fernandes, J. L. Champagneux, R. B. Myneni, J. M. Chen, S. Plummer, M. Weiss, C. Bacour, S. Garrigues, and J. E. Nickeson (2006), Evaluation of the representativeness of networks of sites for the global validation and intercomparison of land biophysical products: Proposition of the CEOS-BELMANIP, *IEEE Trans. Geosci. Remote Sens.*, *44*, 1794–1803.
- Baret, F., et al. (2007), LAI, fAPAR, and fCover CYCLOPES global products derived from VEGETATION: Part 1. Principles of the algorithm, *Remote Sens. Environ.*, *110*, 275–286.
- Bartholomé, E., and A. S. Belward (2005), GLC2000: A new approach to global land cover mapping from Earth observation data, *Int. J. Remote Sens.*, *26*, 1959–1977.
- Bonan, G. B. (1993), Physiological controls of the carbon balance of boreal forest ecosystems, *Can. J. Forest Res.*, *23*, 1453–1471.
- Bond-Lamberty, B., and S. T. Gower (2007), Estimation of stand-level leaf area for boreal bryophytes, *Oecologia*, *151*, 584–592.
- Brown, L. J., J. M. Chen, S. G. Leblanc, and J. Cihlar (2000), Short wave infrared correction to the simple ratio: an image and model analysis, *Remote Sens. Environ.*, *71*, 16–25.
- Bubier, J. L., B. N. Rock, and P. M. Crill (1997), Spectral reflectance measurements of boreal wetland and forest mosses. *J. Geophys. Res.*, *102*(D24), 29,483–29,494, doi:10.1029/97JD02316.
- Buermann, W., J. Dong, X. Zeng, R. B. Myneni, and R. E. Dickinson (2001), Evaluation of the utility of satellite based vegetation leaf area index data for climate simulations, *J. Clim.*, *14*, 3536–3550.
- Burrows, S. N., S. T. Gower, M. K. Clayton, D. S. Mackay, D. E. Ahi, J. M. Norman, and G. Diak (2002), Application of geostatistics to characterize LAI for flux towers to landscapes, *Ecosystems*, *5*, 667–679.
- Canadell, J. G., C. Le Quéré, M. R. Raupach, C. B. Field, E. T. Buitenhuis, P. Ciais, T. J. Conway, N. P. Gillett, R. A. Houghton, and G. Marland (2007), Contributions to accelerating atmospheric CO<sub>2</sub> growth from economic activity, carbon intensity, and efficiency of natural sinks, *Proc. Natl. Acad. Sci. U. S. A.*, *104*, 18,866–18,870.
- CEOS (2006), CEOS response to the GCOS implementation plan, accepted by the UNFCCC November, 2006, (available at <http://lpvs.gsfc.nasa.gov>)
- Chen, J. M. (1996), Optically-based methods for measuring seasonal variation in leaf area index of boreal conifer forests, *Agric. For. Meteorol.*, *80*, 135–163.
- Chen, J. M., and T. A. Black (1992), Defining leaf area index for non-flat leaves, *Plant Cell Environ.*, *15*, 421–429.
- Chen, J. M., and J. Cihlar (1997), A hotspot function in a simple bidirectional reflectance model for satellite applications, *J. Geophys. Res.*, *102*(D22), 25,907–25,913, doi:10.1029/97JD02010.
- Chen, J. M., and S. G. Leblanc (1997), A four-scale bidirectional reflectance model based on canopy architecture, *IEEE Trans. Geosci. Remote Sens.*, *35*, 1316–1337.
- Chen, J. M., and S. G. Leblanc (2001), Multiple-scattering scheme useful for geometric optical modeling, *IEEE Trans. Geosci. Remote Sens.*, *39*, 1061–1071.
- Chen, J. M., P. D. Blanken, T. A. Black, M. Guilbeault, and S. Chen (1997a), Radiation regime and canopy architecture in a boreal aspen forest, *Agric. For. Meteorol.*, *86*, 107–125.
- Chen, J. M., P. M. Rich, S. T. Gower, J. M. Norman, and S. Plummer (1997b), Leaf area index of boreal forests: Theory, techniques and measurements, *J. Geophys. Res.*, *102*(D24), 29,429–29,443, doi:10.1029/97JD01107.
- Chen, J. M., S. G. Leblanc, J. R. Miller, J. Freemantle, S. E. Loebel, C. L. Walthall, K. A. Innanen, and H. P. White (1999), Compact Airborne Spectrographic Imager (CASI) used for mapping biophysical parameters of boreal forests, *J. Geophys. Res.*, *104*(D22), 27,945–27,958, doi:10.1029/1999JD900098.
- Chen, J. M., et al. (2002), Validation of Canada-wide leaf area index maps using ground measurements and high and moderate resolution satellite imagery, *Remote Sens. Environ.*, *80*, 165–184.
- Chen, J. M., C. H. Menges, and S. G. Leblanc (2005), Global mapping of foliage clumping index using multi-angular satellite data, *Remote Sens. Environ.*, *97*, 447–457.
- Chen, J. M., F. Deng, and M. Chen (2006a), Locally adjusted cubic-spline capping for reconstructing seasonal trajectories of a satellite-derived surface parameter, *IEEE Trans. Geosci. Remote Sens.*, *44*, 2230–2238.
- Chen, J. M., A. Govind, O. Sonnentag, Y. Zhang, A. Barr, and B. Amiro (2006b), Leaf area index measurements at Fluxnet-Canada forest sites, FCN special issue, *Agric. For. Meteorol.*, *140*, 257–268.
- Cihlar, J., H. Ly, Z. Li, J. M. Chen, H. Pokrant, and F. Huang (1997), Multitemporal, multichannel AVHRR data sets for land biosphere studies: Artifacts and corrections, *Remote Sens. Environ.*, *60*, 35–57.
- Cohen, W. B., T. K. Maierberger, Z. Yang, S. T. Gower, D. P. Turner, W. D. Ritts, M. Berterretche, and S. W. Running (2003), Comparisons of land cover and LAI estimates derived from ETM+ and MODIS for four sites in North America: A quality assessment of 2000/2001 provisional MODIS products, *Remote Sens. Environ.*, *88*, 233–255.
- Cohen, W. B., T. K. Maierberger, and D. Pflugmacher (2006a), BigFoot Land Cover Surfaces for North and South American Sites, 2000–2003, <http://www.daac.ornl.gov>, Oak Ridge Natl. Lab. Distrib. Active Arch. Cent., Oak Ridge, Tenn.
- Cohen, W. B., T. K. Maierberger, D. P. Turner, W. D. Ritts, D. Pflugmacher, R. E. Kennedy, A. Kirschbaum, S. W. Running, M. Costa, and S. T. Gower (2006b), MODIS land cover and LAI Collection 4 product quality across nine sites in the Western Hemisphere, *IEEE Trans. Geosci. Remote Sens.*, *44*, 1843–1857.
- Deng, D., J. M. Chen, S. Plummer, M. Chen, and J. Pisek (2006), Global LAI algorithm integrating the bidirectional information, *IEEE Trans. Geosci. Remote Sens.*, *44*, 2219–2229.
- Deschamps, P. Y., F. M. Breon, M. Leroy, A. Podaire, A. Bricaud, J. C. Buriez, and G. Seze (1994), The POLDER mission: instrument characteristics and scientific objectives, *IEEE Trans. Geosci. Remote Sens.*, *32*, 598–615.
- Diner, D. J., J. C. Beckert, T. H. Reilly, C. J. Bruegge, J. E. Conel, R. A. Kahn, J. V. Martonchik, T. P. Ackerman, R. Davies, S. A. W. Gerstl, H. R. Gordon, J. -P. Muller, R. B. Myneni, P. J. Sellers, B. Pinty, and M. M. Verstraete (1998), Multi-angle imaging spectro-radiometer

- (MISR) instrument description and experiment overview, *IEEE Trans. Geosci. Remote Sens.*, 36, 1072–1087.
- Eriksson, H., L. Eklundh, A. Kuusk, and T. Nilson (2006), Impact of understory vegetation on forest canopy reflectance and remotely sensed LAI estimates, *Remote Sens. Environ.*, 103, 408–418.
- Fensholt, R., I. Sandholt, and M. S. Rasmussen (2004), Evaluation of MODIS LAI, fAPAR and the relation between fAPAR and NDVI in a semi-arid environment using in situ measurements, *Remote Sens. Environ.*, 91, 490–507.
- Fillol, E., F. Baret, M. Weiss, G. Dedieu, V. Demarez, P. Gouaux, and D. Ducrot (2006), Cover fraction estimation from high resolution SPOT HRV&HRG and medium resolution SPOT-VEGETATION sensors. Validation and comparison over South-West France, in *Proceedings of the Second International Symposium on Recent Advances in Quantitative Remote Sensing*, edited by J. Sobrino, pp. 659–663, Univ. of Valencia, Valencia, Spain.
- Garrigues, S., et al. (2008), Validation and intercomparison of global Leaf Area Index products derived from remote sensing data, *J. Geophys. Res.*, 113, G02028, doi:10.1029/2007JG000635.
- Gemmell, F. (2000), Testing the utility of multi-angle spectral data for reducing the effects of background spectral variations in forest reflectance model inversion, *Remote Sens. Environ.*, 72, 46–63.
- Goward, S. N., K. F. Huemmrich, and R. H. Waring (1994), Visible-near infrared spectral reflectance of landscape components in western Oregon, *Remote Sens. Environ.*, 47, 190–203.
- Gower, S. T., J. G. Vogel, J. M. Norman, C. J. Kucharik, S. J. Steele, and T. K. Stow (1997), Carbon distribution and aboveground net primary production in aspen, jack pine, and black spruce stands in Saskatchewan and Manitoba, Canada, *J. Geophys. Res.*, 102(D24), 29,029–29,041, doi:10.1029/97JD02317.
- Gower, S. T., C. J. Kucharik, and J. M. Norman (1999), Direct and indirect estimation of leaf area index, fAPAR, and net primary production of terrestrial ecosystems, *Remote Sens. Environ.*, 70, 29–51.
- Iames, J., R. Congalton, A. Pilant, and T. Lewis (2008), Leaf area index (LAI) change detection analysis on Loblolly Pine (*Pinus taeda*) following complete understory removal, *Photogramm. Eng. Remote Sens.*, 74, 1389–1400.
- Jonckheere, I., S. Fleck, K. Nackaerts, B. Muys, P. Coppin, M. Weiss, and F. Baret (2004), Review of methods for in situ leaf area index determination: Part I. Theories, sensors and hemispherical photography, *Agric. For. Meteorol.*, 121, 19–35.
- Knyazikhin, Y., J. V. Martonchik, D. J. Diner, R. B. Myneni, M. M. Verstraete, B. Pinty, and N. Gobron (1998a), Estimation of vegetation canopy leaf area index and fraction of absorbed photosynthetically active radiation from atmosphere corrected MISR data, *J. Geophys. Res.*, 103(D24), 32,239–32,256, doi:10.1029/98JD02461.
- Knyazikhin, Y., J. V. Martonchik, R. B. Myneni, D. J. Diner, and S. W. Running (1998b), Synergistic algorithm for estimating vegetation canopy leaf area index and fraction of absorbed photosynthetically active radiation from MODIS and MISR data, *J. Geophys. Res.*, 103(D24), 32,257–32,275, doi:10.1029/98JD02462.
- Kobayashi, H., N. Delbart, R. Suzuki, and K. Kushida (2010), A satellite-based method for monitoring seasonality in the overstory leaf area index of Siberian larch forest, *J. Geophys. Res.*, 115, G01002, doi:10.1029/2009JG000939.
- Kuusk, A., M. Lang, and T. Nilson (2004), Simulation of the reflectance of ground vegetation in sub-boreal forests, *Agric. For. Meteorol.*, 126, 33–46.
- Lang, M., T. Nilson, A. Kuusk, A. Kiviste, and M. Hordo (2007), The performance of foliage mass and crown radius models in forming the input of a forest reflectance model: A test on forest growth sample plots and Landsat 7 ETM+ images, *Remote Sens. Environ.*, 110, 445–457.
- Law, B. E., S. Van Tuyl, A. Cescatti, and D. D. Baldocchi (2001), Estimation of leaf area index in open-canopy ponderosa pine forests at different successional stages and management regimes in Oregon, *Agric. For. Meteorol.*, 108, 1–14.
- Lundmark, T., J. Hallgren, and J. Heden (1988), Recovery from winter depression of photosynthesis in pine and spruce, *Trees*, 2, 110–114.
- Magill, A. H., et al. (2004), Ecosystem response to 15 years of chronic nitrogen additions at the Harvard Forest LTER, Massachusetts, USA, *For. Ecol. Manage.*, 196, 7–28.
- Miller, J., et al. (1997), Seasonal change in understory reflectance of boreal forests and influence on canopy vegetation indices, *J. Geophys. Res.*, 102(D24), 29,475–29,482, doi:10.1029/97JD02558.
- Morisette, J. T., et al. (2006), Validation of global moderate-resolution LAI products: A framework proposed within the CEOS Land Product Validation subgroup, *IEEE Trans. Geosci. Remote Sens.*, 44, 1804–1817.
- Myneni, R. B., R. R. Nemani, and S. W. Running (1997), Estimation of global leaf area index and absorbed par using radiative transfer models, *IEEE Trans. Geosci. Remote Sens.*, 35, 1380–1393.
- Myneni, R. B., Y. Knyazikhin, J. L. Privette, J. Glassy, Y. Tian, Y. Zhang, J. T. Morisette, R. R. Nemani, and S. W. Running (2002), Global products of vegetation leaf area and fraction absorbed PAR from year one of MODIS data, *Remote Sens. Environ.*, 83, 214–231.
- Nilson, T. (1971), A theoretical analysis of the frequency of gaps in plant stands, *Agric. Meteorol.*, 8, 25–38.
- Pisek, J., and J. M. Chen (2007), Comparison and validation of MODIS and VEGETATION global LAI products over four BigFoot sites in North America, *Remote Sens. Environ.*, 109, 81–94.
- Pisek, J., and J. M. Chen (2009), Mapping forest background reflectivity over North America with Multi-angle Imaging SpectroRadiometer (MISR), *Remote Sens. Environ.*, 113(11), 2412–2423, doi:10.1016/j.rse.2009.07.003.
- Pisek, J., J. M. Chen, and F. Deng (2007), Assessment of a new global leaf area index dataset from SPOT-4 VEGETATION data over selected sites in Canada, *Can. J. Remote Sens.*, 33, 341–356.
- Pisek, J., J. M. Chen, R. Lacaze, O. Sonnentag, and K. Alikas (2010a), Refining global mapping of foliage clumping index with multi-angular POLDER 3 measurements: Evaluation and topographic compensation, *ISPRS J. Photogramm. Remote Sens.*, 65, 341–346.
- Pisek, J., J. M. Chen, J. R. Miller, J. R. Freemantle, J. I. Peltoniemi, and A. Simic (2010b), Mapping forest background reflectance in a boreal region using multiangle Compact Airborne Spectrographic Imager (CASI) data, *IEEE Trans. Geosci. Remote Sens.*, 48(1), 499–510, doi:10.1109/TGRS.2009.2024756.
- Pocewicz, A., L. Vierling, L. Lentile, and R. Smith (2007), View angle effects on relationships between MISR vegetation indices and leaf area index in a recently burned ponderosa pine forest, *Remote Sens. Environ.*, 107, 322–333.
- Rautiainen, M., et al. (2007), Coupling forest canopy and understory reflectance in the Arctic latitudes of Finland, *Remote Sens. Environ.*, 110, 332–343.
- Rentch, J. S., M. A. Fajvan, and R. R. Hicks Jr. (2003), Oak establishment and canopy accession strategies in five old-growth stands in the central hardwood forest region, *For. Ecol. Manage.*, 184, 285–297.
- Ross, M. S., L. B. Flanagan, and G. H. La Roi (1986), Seasonal and successional changes in light quality and quantity in the understory of boreal forest ecosystems, *Can. J. Bot.*, 64, 2792–2799.
- Roujean, J. L., M. Leroy, and P. Y. Deschamps (1992), A bidirectional reflectance model of the earth's surface for the correction of remote sensing data, *J. Geophys. Res.*, 97(D18), 20,455–20,468, doi:10.1029/92JD01411.
- Sellers, P. J., D. A. Randall, G. J. Collatz, J. A. Berry, C. B. Field, D. A. Dazlich, C. Zhang, G. D. Collelo, and L. Bounoua (1996), A revised land surface parameterization (SIB2) for atmospheric GCMs: Part I. Model formulation, *J. Clim.*, 9, 676–705.
- Serbin, S. P., S. T. Gower, and D. E. Ahl (2009), Canopy dynamics and phenology of a boreal black spruce wildfire chronosequence, *Agric. For. Meteorol.*, 149, 187–204.
- Shabanov, N. V., et al. (2005), Optimization of the MODIS LAI and FPAR algorithm performance over broadleaf forests, *IEEE Trans. Geosci. Remote Sens.*, 43, 1855–1865.
- Sonnentag, O., J. M. Chen, D. A. Roberts, J. Talbot, K. Q. Halligan, and A. Govind (2007), Mapping tree and shrub leaf area indices in an ombrotrophic peatland through multiple endmember spectral unmixing, *Remote Sens. Environ.*, 109, 342–360.
- Steinberg, D. C., S. J. Goetz, and E. J. Hyer (2006), Validation of MODIS FPAR products in boreal forests of Alaska, *IEEE Trans. Geosci. Remote Sens.*, 44, 1818–1828.
- Stenberg, P., M. Rautiainen, T. Manninen, P. Voipio, and H. Smolander (2004), Reduced simple ratio better than NDVI for estimating LAI in Finnish pine and spruce stands, *Silva Fennica*, 38, 3–14.
- Strand, M., and T. Lundmark (1995), Recovery of photosynthesis in 1-year-old needles of unfertilized and fertilized Norway spruce (*Picea abies* (L.) Karst.) during spring, *Tree Physiol.*, 15, 151–158.
- Verger, A., F. Camacho-de Coca, and J. Meliá (2006), Inter-comparison of algorithms for retrieving operationally vegetation parameters at global scale: Assessment over Europe along 2003, in *Proceedings of the Second International Symposium on Recent Advances in Quantitative Remote Sensing, Sep. 2006*, edited by J. Sobrino, pp. 909–914, Univ. of Valencia, Valencia, Spain.
- Verger, A., F. Baret, and M. Weiss (2008), Performances of neural networks for deriving LAI estimates from existing CYCLOPES and MODIS products, *Remote Sens. Environ.*, 112, 2789–2803.
- Vogel, J. S., and S. T. Gower (1998), Carbon dynamics of boreal jack pine stands with and without a green alder understory, *Ecosystems*, 1, 386–400.
- Wang, Y., Y. Tian, Y. Zhang, N. El-Saleous, Y. Knyazikhin, E. Vermote, and R. B. Myneni (2001), Investigation of product accuracy as a function

- of input and model uncertainties: Case study with SeaWiFS and MODIS LAI/FPAR algorithm, *Remote Sens. Environ.*, *78*, 296–311.
- Weiss, M., F. Baret, G. J. Smith, I. Jonckheere, and P. Coppin (2004), Review of methods for in situ leaf area index (LAI) determination: Part II. Estimation of LAI, errors and sampling, *Agric. For. Meteorol.*, *121*, 37–53.
- Weiss, M., F. Baret, S. Garrigues, and R. Lacaze (2007), LAI and fAPAR CYCLOPES global products derived from VEGETATION: Part 2. Validation and comparison with MODIS Collection 4 products, *Remote Sens. Environ.*, *110*, 317–331.
- Yang, W., et al. (2006a), MODIS leaf area index products: From validation to algorithm improvement, *IEEE Trans. Geosci. Remote Sens.*, *44*, 1885–1898.
- Yang, W., N. V. Shabanov, D. Huang, W. Wang, R. E. Dickinson, R. R. Nemani, Y. Knyazikhin, and R. B. Myneni (2006b), Analysis of leaf area index products from combination of MODIS Terra and Aqua data, *Remote Sens. Environ.*, *104*, 297–312.
- Zhang, Y., J. M. Chen, J. R. Miller, and T. L. Noland (2008), Retrieving chlorophyll content in conifer needles from hyperspectral measurements, *Can. J. Remote Sens.*, *34*, 296–310.
- 
- J. M. Chen, F. Deng, and J. Pisek, Department of Geography and Program in Planning, University of Toronto, Toronto, ON M5S 3G3, Canada. (jan.pisek@utoronto.ca)
- K. Alikas, Tartu Observatory, 61602 Tõravere, Estonia.